(p)ppGpp and malonyl-CoA set the pace for *Staphylococcus aureus* adaptation to FASII antibiotics and provide a basis for bi-therapy inhibition

Amit Pathania[1*], Jamila Anba-Mondoloni[1], David Halpern[1], Laëtitia Dupont[1], Gilles Lamberet[1], Patrick Trieu-Cuot [2], Karine Gloux[1] and Alexandra Gruss[1*]

[1]Micalis Institute, INRAE, AgroParisTech, Université Paris-Saclay, Jouy en Josas, France, [2] Unité de Biologie des Pathogènes à Gram-positif, CNRS UMR 2001, Institut Pasteur, Paris, France

* For correspondence:

amit.pathania@inrae.fr ORCID 0000-0003-2304-5060

alexandra.gruss@inrae.fr ORCID 0000-0001-7426-5229

Keywords: FASII adaptation, (p)ppGpp, malonyl-CoA, phospholipids, antibiotic bi-therapy, triclosan, AFN-1252, mupirocin

Abstract

Fatty acid biosynthesis (FASII) enzymes have been considered as valid targets for antimicrobial drug development against the human pathogen *Staphylococcus aureus*. However, incorporation of host fatty acids confers FASII antibiotic adaptation that compromises prospective treatments. *S. aureus* adaptation to FASII inhibitors is preceded by a non-replicative latency period. Here we investigated the factors that dictate the duration of latency prior to adaptation outgrowth, and identify stringent response as a regulator of both FASII and adaptation to FASII inhibition. We show that in addition to the FapR repressor, (p)ppGpp induction inhibits malonyl-CoA synthesis, and constitutes a second regulator of FASII and phospholipid synthesis in *S. aureus*. Anti-FASII treatment triggers transient (p)ppGpp induction during the anti-FASII latency phase, with a concomitant reduction of FapR regulon expression. This effect is reversed upon adaptive outgrowth. Results indicate that anti-FASII treatment shifts malonyl-CoA distribution between its interactants, FapR and FabD, increasing expression of phospholipid synthesis genes *plsX* and *plsC* during outgrowth. We conclude that (p)ppGpp pools dictate malonyl-CoA availability in *S. aureus* FASII regulation, and contribute to latency prior to anti-FASII adaptation. A combinatory approach, coupling a (p)ppGpp inducer and an anti-FASII, blocks *S. aureus* growth, opening perspectives for bi-therapy treatment.

45 **Introduction**

46 Bacterial infections that fail to respond to antibiotic treatments are on the rise, especially in the
47 immunocompromised or weakened host, underlining the need for novel antimicrobial strategies [1].
48 The fatty acid synthesis (FASII) enzymes were considered as fail-safe targets for eliminating
49 numerous Gram-positive pathogens. Anti-FASII has been a front-line drug against *Mycobacterium*
50 *tuberculosis*, which synthesize very long chain fatty acids that cannot be compensated by the
51 environment [2]. However, firmicute pathogens, including *Staphylococcus aureus* and numerous
52 streptococcaceae, bypass FASII inhibition and satisfy their fatty acid requirements by using host-
53 supplied fatty acids [3-5]. FASII inhibitors like triclosan (Tric), MUT056399, fasamycins A and B,
54 amycomicin and AFN-1252 [6-11], would thus have limited use as stand-alone treatments of infections
55 by numerous Gram-positive pathogens [3-5].

56 Our recent studies show that *S. aureus* may adapt to FASII inhibitors by two mechanisms,
57 depending on growth conditions. One involves mutations in a FASII initiation gene (usually *fabD*): a
58 FabD mutant with decreased affinity for acyl carrier protein (ACP) would increase ACP availability for
59 incorporation of exogenous fatty acids (eFA) *via* the phosphate acyltransferase PlsX (Fig. S1) [4,12]. The
60 second mode of adaptation occurs without FASII mutations and predominates in serum-
61 supplemented medium. In this case, full adaptation and eFA incorporation in actively growing cells is
62 achieved after a latency phase, whose duration (6-12 h) depends on the strain and pre-growth
63 conditions. Adaptation is associated with greater intracellular retention of eFA and ACP, which both
64 contribute to eFA incorporation in membrane phospholipids to compensate FASII inhibition [5].

65 The factors regulating *S. aureus* transition between latency and adaptation to anti-FASII
66 remain unknown. We hypothesized that initial fatty acid bacterial starvation in response to anti-FASII
67 might comprise the signal that delays exogenous fatty acid compensation in the latency period prior
68 to outgrowth. The *S. aureus* FapR protein regulates most FASII genes (except *acc*, encoding acetyl-
69 CoA carboxylase, and FabZ, β-hydroxyacyl-ACP dehydratase), and also phospholipid synthesis genes
70 *plsX* and *plsC* [13,14]. Interestingly, malonyl-CoA, the first dedicated FASII substrate used by FabD
71 (malonyl-CoA transacylase), also controls the FapR repressor by a feed-forward mechanism [14]. FabD
72 uses malonyl-CoA, together with ACP, to synthesize malonyl-ACP [15]. Malonyl-CoA binding to FapR
73 reverses FapR repression, leading to up-regulation of most FASII genes and phospholipid synthesis
74 genes *plsX* and *plsC* [14]. These observations point out roles for malonyl-CoA in both enzymatic and
75 regulatory activities of FASII. In *Escherichia coli*, expression of the malonyl-CoA synthesis enzyme ACC
76 is regulated by (p)ppGpp, which accumulates in slow growing, nutrient-deficient conditions [16,17];
77 (p)ppGpp also reportedly regulates other FASII, and phospholipid synthesis genes [18,19]. In *B. subtilis*,
78 fatty acid starvation triggers activation of the stringent response [20] and is associated with cell size *via*

79 regulation of FASII, although the mechanism remains to be elucidated [21]. To our knowledge, no
80 evidence exists for (p)ppGpp-mediated FASII regulation in *S. aureus*.

81 Here, we first show that (p)ppGpp exerts a second level of FASII regulation in *S. aureus*. We
82 report that (p)ppGpp synthesis is induced during FASII-antibiotic-induced latency, prior to
83 adaptation. The chain of events revealed here indicate that (p)ppGpp and malonyl-CoA regulate the
84 timing of FASII-antibiotic-induced latency transition to adaptation. Based on these findings, we
85 suggest a bi-therapy approach that combines FASII inhibitors and a (p)ppGpp inducer to prevent *S.*
86 *aureus* adaptation.

87

88 **Results**

89 **(p)ppGpp negatively regulates malonyl-CoA levels in *S. aureus*.**

90 We investigated the potential roles of (p)ppGpp and malonyl-CoA in response to FASII inhibition.
91 Previous studies reported difficulties in (p)ppGpp measurements in *B. subtilis* and *S. aureus* [20,22]. Our
92 initial attempts at measuring (p)ppGpp by HPLC and fluorescent dye PyDPA [23] failed to give reliable
93 results (data not shown). We therefore constructed and validated tools for *in vivo* (p)ppGpp
94 detection (Table S1). Stringent-response-sensitive promoters were confirmed to be up-regulated
95 (P_{oppB}-*lacZ*; NWMN_0856, P_{ilvD}-*lacZ* NWMN_1960) or down-regulated (P_{cshA}-*lacZ*; NWMN_1985) [24], by
96 mupirocin, which inhibits isoleucyl-tRNA synthetase [24]. As all results with P_{oppB}-*lacZ* were comparable
97 to those with P_{ilvD}-*lacZ*, only the first is presented in experiments below. The reporter fusion activities
98 responded to mupirocin as expected (Fig. 1A; Materials and Methods). Nutrient starvation during
99 stationary phase induces stringent response in *Escherichia coli* [16]. Accordingly, β-galactosidase (β-gal)
100 activity of the P_{oppB}-*lacZ* sensor was ~7-fold higher in stationary phase compared to exponential
101 phase cells, while P_{cshA}-*lacZ* activity was ~2-fold lower (Fig. 1B), further validating the *in vivo* (p)ppGpp
102 sensors.

103 We asked whether (p)ppGpp blocks malonyl-CoA synthesis in *S. aureus*, as occurs in *E. coli* [25]**.**
104 Although FASII regulation differs in *S. aureus* [13], (p)ppGpp might have a common effect, as was also
105 suggested in *B. subtilis* [20]. Total malonyl-CoA was measured in cells treated or not with mupirocin by
106 ELISA immunoassay. In addition, expression of *accB accC* (NWMN_1432 and NWMN_1431), encoding
107 the AccB and AccC subunits of acetyl-CoA carboxylase (ACC), was followed using *in vivo* promoter
108 fusion P_{accBC}-*lacZ* (Table S1). Stringent response induction by mupirocin led to decreases in malonyl-
109 CoA pools (~6-fold) and in P_{accBC}-*lacZ* β-gal activity (~4-fold) (Fig. 1C). Similarly, stationary phase cells
110 showed lower production of malonyl-CoA and P_{accBC}-*lacZ* β-gal activity compared to exponential

111 phase cells (Fig. 1D). These results indicate a link between (p)ppGpp and FASII, missing until now in *S.*
112 *aureus*.

113 **Expression of (p)ppGpp-regulated genes is transiently increased during FASII-antibiotic-induced**
114 **latency and diminished during outgrowth.**

115 We recently showed that host fatty acids can compensate FASII-antibiotic inhibition of *S. aureus* to
116 promote growth. Adaptation occurs without FASII mutations in conditions of low membrane stress as
117 in serum, following an initial latency phase ([5]; Fig. 2A). Once adapted to anti-FASII, *S. aureus* fatty acid
118 profiles are fully exogenous (Fig. S1B). As anti-FASII treatment may provoke fatty acid deprivation
119 before exogenous fatty acids are incorporated, we asked whether the latency preceding FASII bypass
120 corresponds to stringent response induction. Using the stringent response sensors, a ~3-fold increase
121 in P_{oppB}-*lacZ* and ~7-fold decrease of P_{cshA}-*lacZ* β-gal activities were observed during the latency phase
122 preceding outgrowth (Fig. 2B), indicating that stringent response is induced probably due to
123 insufficient incorporation of fatty acids. Importantly, P_{oppB}-*lacZ* activity in adaptive exponential
124 outgrowth cells was similar to that measured in exponential growing cells without triclosan. P_{cshA}-*lacZ*
125 β-gal activity in adaptive exponential outgrowth cells is 2-fold that observed during latency, although
126 it remains 3.5-fold less than that observed without triclosan.

127 We examined previously published proteomes of *S. aureus* isolates in mupirocin, and noted
128 that numerous responses overlapped with those observed in anti-FASII latency ([5]**;** DOI:
129 10.17632/9292c75797.2; [24,26], and Table S2). While the strains used in those analyses were different,
130 the observed responses are in conserved genes and could reasonably be expected to be maintained
131 across species. Altogether, these data support a role for (p)ppGpp in response to FASII inhibitor
132 treatment during the latency phase.

133 **FASII antibiotic treatment impacts FapR activity and malonyl-CoA levels.**

134 We considered that malonyl-CoA availability and/or distribution between its two known interactants
135 FapR and FabD ([27] and Fig. 3A) might be involved in modulating eFA incorporation and anti-FASII
136 adaptation. To test this, we evaluated malonyl-CoA pools in different ways: ELISA assays and a P_{accB}-
137 *lacZ* reporter give information on total malonyl-CoA pools (see Fig. 1C,D). We also designed a FapR
138 sensor (FapR-Trap; Fig. S2A), as previously used to estimate malonyl-CoA pools in bacteria [28-30]
139 (Materials and Methods, Table S1). In fact, this sensor measures malonyl-CoA that is bound to FapR.
140 As expected, β-gal activity of FapR-Trap was up-regulated (5-fold) in a *fapR* deletion strain compared
141 to the isogenic WT strain (RN4220; Fig. S2B).

142 Evaluation of malonyl-CoA pools in non-selective and SerFA-Tric latency and outgrowth
143 cultures revealed that both the quantity and availability of malonyl-CoA depend upon growth

144 conditions (Fig. 2). Total cellular malonyl-CoA pools, as measured by ELISA or with the P_{accBC}-*lacZ*
145 fusion, were markedly lower in SerFA-Tric latency cultures when compared to FASII-antibiotic-
146 adapted *S. aureus* and in SerFA control cultures. However, non-selective and adapted cultures
147 showed comparable amounts of malonyl-CoA (Fig. 3C). In sharp contrast, malonyl-CoA estimations by
148 FapR-Trap were around 10-fold higher in SerFA-Tric adapted, compared to non-selective SerFA
149 cultures (compare Fig. 3B and 3C). These findings indicate that unlike control SerFA growth, malonyl-
150 CoA distribution during FASII antibiotic adaptation favors FapR binding. Proportionately greater FapR
151 binding is already detected in the latency phase; while total malonyl-CoA levels were ~4-fold lower in
152 the latency culture than in the SerFA control, FapR-Trap induction levels were equivalent. These
153 observed differences (summarized in Table S3) suggest that malonyl-CoA pools and their distribution
154 between FapR and FabD may be central determinants in regulating adaptation to FASII antibiotics.

155 We reported that *fabD* mutants often emerge upon FASII-antibiotic selection, but not in
156 serum-supplemented medium as used here [4,5]. Reduced FabD activity would increase malonyl-CoA
157 availability for FapR (Fig. S1). Consistent with this reasoning and previous findings, a *fabD* mutant
158 displayed 5-fold greater FapR-Trap expression than the parental strain in non-selective SerFA (Fig.
159 3D). However, we ruled out the presence of *fabD* mutations in our conditions by DNA sequencing of
160 5 independent anti-FASII-adapted cultures (performed using the same strain and SerFA-Tric
161 erythromycin conditions, and a control without triclosan; data not shown). These findings could
162 suggest that FabD is intact, but disabled for its interactions with malonyl-CoA during *S. aureus* growth
163 in the presence of anti-FASII. This possibility is currently under study in our laboratory.

164 **Expression of phospholipid synthesis genes *plsX* and *plsC* is up-regulated in FASII-antibiotic-**
165 **adapted *S. aureus*.**

166 The above results show that malonyl-CoA pools are restored during *S. aureus* adaptation to FASII
167 antibiotics, and preferentially bind FapR. Increased malonyl-CoA de-represses FapR-controlled genes,
168 including *plsX* (NWMN_1139, part of the *fapR* operon) and *plsC* (NWMN_1620) ([13]; Fig. 4A). FASII
169 antibiotic adaptation presumably requires expression of both genes (Fig. S1). We therefore used
170 reporter fusions to *plsX* and *plsC* promoters (respectively $P_{fapR\ plsX}$-*lacZ* and P_{plsC}-*lacZ*, Table S1) to
171 follow gene expression during anti-FASII-induced latency and outgrowth. $P_{fapR\ plsX}$-*lacZ* and P_{plsC}-*lacZ*
172 expression gradually decreased during latency, followed by abrupt (respectively 4-fold and 2-fold)
173 increases upon restart of active growth of FASII-antibiotic-adapted cells (Fig. 4B and 4C, and data not
174 shown). Expression of *plsX* from $P_{fapR\ plsX}$-*lacZ* was even higher (~3-fold) in anti-FASII adaptive
175 outgrowth than in non-selective growth (Fig. 3).

176

177 **Mupirocin inhibits *S. aureus plsX* and *plsC* expression and eFA incorporation, and acts**
178 **synergistically with FASII antibiotics to block growth.**

179 A main objective of this study was to determine whether (p)ppGpp induction affects eFA
180 incorporation in phospholipids, a requisite for anti-FASII adaptation. To answer this question, we
181 blocked malonyl-CoA synthesis by inducing the stringent response with mupirocin (0.1 µg/ml), and
182 then followed *plsX* and *plsC* expression, using as controls the known stringent response genes (Table
183 S4). A 4- and 3-fold repression was observed for respectively *plsX* and *plsC* sensor fusions in the
184 presence of mupirocin, which was similar to repression of the *cshA* down-regulated control.

185 The impact of stringent response induction on fatty acid profiles was then examined. *S.*
186 *aureus* Newman was grown in SerFA without and with sublethal mupirocin addition (0.05 µg/ml, 5-
187 fold below the MIC; [31]). Fatty acid profiles of the exponential cultures were compared 3 h post-
188 treatment showed 15% lower eFA incorporation in mupirocin-treated compared to non-treated
189 cultures (Fig. 5A). This is consistent with the above results showing that stringent response lowers
190 *plsX* and *plsC* expression (Table S4). We recently reported poor eFA incorporation during anti-FASII
191 latency [5]**.** (p)ppGpp induction during anti-FASII-induced latency could thus slow or stop eFA
192 incorporation in this transient period.

193 The above findings led us to hypothesize that FASII inhibitors could be synergistic with a
194 stringent response inducer that prevents compensatory eFA incorporation by repressing
195 phospholipid synthesis genes *plsX* and *plsC* (Fig. 4B and Table S4). Addition of a subinhibitory
196 concentration of mupirocin (0.05 µg/ml) to *S. aureus* SerFA-Tric cultures resulted in extended
197 latency, whereas neither mupirocin nor triclosan separately blocked bacterial growth (**Fig. 5B**).
198 Similar results were obtained using an MRSA (USA300 FPR3757) coupled to a pipeline FASII antibiotic
199 AFN-1252 [7] (Table S5). The observed synergistic effect between two flawed antibiotics may offer an
200 effective strategy for development of last-resort treatments against *S. aureus* infection.

201

202 **Discussion**

203 FapR is to date the main known FASII regulator in *S. aureus*. Here we identify (p)ppGpp as a second
204 *S. aureus* FASII regulator, which represses *accB accC* expression and lowers malonyl-CoA levels. Thus,
205 despite differences in FASII regulation between *S. aureus* and *E. coli*, (p)ppGpp appears to have a
206 common role in these species ([25], this report). Our results further show that (p)ppGpp regulation of
207 FASII impacts the duration of the latency phase preceding adaptation to a FASII block. We propose
208 that (p)ppGpp induction is a response to anti-FASII-induced lipid starvation prior to compensation
209 with eFA, although the specific inducer remains to be identified. By repressing *acc*, stringent
210 response induction sets off a chain of events leading to transient repression of the FapR regulon
211 comprising phospholipid synthesis genes *plsX* and *plsC* (Fig. 4). It also correlates with limited eFA
212 incorporation, which may be directly responsible for latency (Fig. 5A). Upon *S. aureus* adaptive
213 outgrowth, (p)ppGpp levels decrease, allowing eFA incorporation and adaptation to FASII antibiotics.
214 These results suggest a model (Fig. 6) in which (p)ppGpp modulation of malonyl-CoA pools controls
215 expression of phospholipid enzymes and sets the timing of anti-FASII adaptation outgrowth.

216 This study uncovers a new role for malonyl-CoA in anti-FASII adaptation *via* its increased
217 association with FapR in antibiotic-adapted cultures compared to non-selective cultures (Fig. 3). The
218 FapR-regulon shows ~10-fold greater expression in anti-FASII-adapted cultures than in non-selective
219 cultures, despite comparable total malonyl-CoA pools (Fig. 3, Fig. 6). Increased malonyl-CoA
220 interaction with FapR during anti-FASII adaptation is consistent with increased *plsX* and *plsC*
221 expression (Fig. 4**)**. Malonyl-CoA rerouting in anti-FASII may be explained by FabD inactivation in anti-
222 FASII adaptation conditions, for example by inhibition *via* an intermediate metabolite as suggested in
223 *E. coli* [32], or by post-translational FabD modification, which modulates FabD stability as reported in
224 *Mycobacterium tuberculosis* [33]. Alternatively, FabD activity may be reversed upon FASII inhibition due
225 to a pile-up of its end-product, malonyl-ACP; however accumulation was not observed in previous
226 study [4]. Finally, an increase in FapR pools might outcompete FabD for malonyl-CoA binding. These
227 hypotheses are now being investigated. These findings indicate limits to the reliability of FapR
228 operon-based sensors to estimate malonyl-CoA pools, for which readouts vary according to growth
229 conditions. This may be important to consider in bioengineering applications that rely on FapR
230 operon-like sensors to optimize malonyl-CoA production [30]**.**

231 The need for antimicrobial alternatives is urgent and, besides the discovery of new molecules
232 or targets, the development of efficient combinations based on existing but poorly effective drugs
233 remains to be explored. Our findings open perspectives for combinatorial antibiotic strategies using
234 FASII inhibitor, and subinhibitory concentrations of drugs that delay or prevent FASII bypass by the
235 major human pathogen *S. aureus*. The proof of concept demonstrated here using anti-FASII

236 antibiotics and mupirocin, suggests a useful bi-therapy approach for reducing *S. aureus* survival
237 during infection.

238

239 **Acknowledgements**

240 We gratefully acknowledge the cooperation of J. Dairou, Université Paris Descartes, France, for HPLC
241 determinations done in initial studies. We are also thankful to Jong-In Hong, Seoul National
242 University, Korea, for the generous gift of PyDPA used in initial studies. Our colleagues P. Bouloc
243 (I2BC, France), C. Morvan (U. Paris-Descartes, France), and MicrobAdapt team members E. Borezée-
244 Durant, D. Lechardeur, G. Kénanian, R. Boudjemaa, and P. Gaudu gave valuable advice. G. Dubey and
245 N. Descoeudres provided kind support. We gratefully acknowledge financial support from DIM-
246 MalInf (AP fellowship), French Agence Nationale de la Recherche (StaphEscape project ANR-
247 13001038) and Fondation pour la Recherche Medicale (DBF20161136769). This work is dedicated to
248 Gilles Lamberet (passed away Dec 23, 2019).

249

250 **Author Contributions**

251 Physiology, molecular biology, (p)ppGpp and malonyl-CoA estimation: AP, PTC, DH. Fatty Acid
252 Profiles: GL, KG and AG. Proteomics analyses: JA-M, LD, JD, AG. Data analyses: AP, JAM, PTC, and AG.
253 Experimental design and project conception: AP and AG. AG directed the project and AP, KG and AG
254 wrote the manuscript.

255

256 **Declaration of Interests**

257 The authors declare no competing interests.

258

259

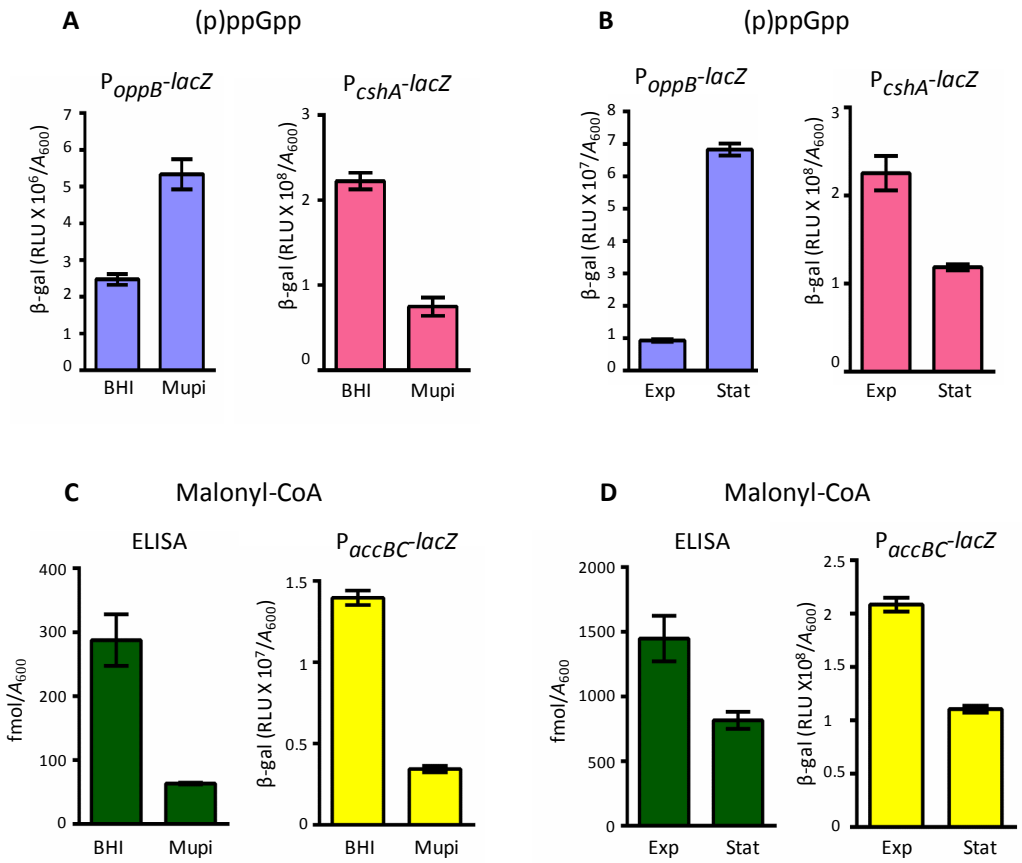

260

261

262 **Fig. 1. Evaluation of (p)ppGpp, malonyl-CoA, and *accBC* activity upon mupirocin treatment (A,C),**
263 **and in exponential (Exp) and stationary (Stat) phases (B,D).** *S. aureus* Newman strains contain
264 reporter systems as indicated. Strains were grown in BHI and BHI containing 0.1 µg/ml mupirocin for
265 1h (**A**,**C**), or in SerFA (A_{600} ~4.0, Exp) and stationary phase (A_{600} ~10.0, Stat) (**B** and **D**). P_{oppB}-*lacZ* and
266 P_{cshA}-*lacZ* expression were evaluated by β-gal assays. Total Malonyl-CoA levels were determined by
267 immunoassay (ELISA; green), and deduced from P_{accBC}-*lacZ* expression (yellow). *opp* and *cshA* genes
268 are respectively up-regulated (blue) and down-regulated (pink) by stringent response induction. See
269 Table S4 for other FapR regulon genes repressed by (p)ppGpp.

270

271

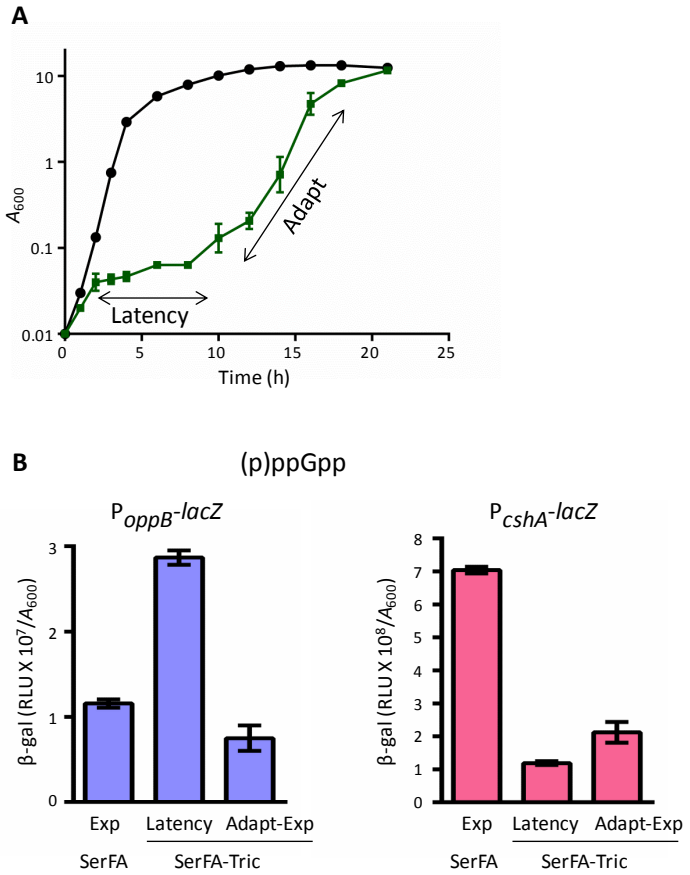

272

273

274 **Fig. 2. Transient *S. aureus* stringent response induction during the latency phase prior to anti-FASII**
275 **adaptation. A.** Growth kinetics of *S. aureus* Newman in BHI (black line) and in SerFA-Tric (green) [5]. In
276 SerFA-Tric, a 10-12 h latency period (Latency) precedes adaptive exponential outgrowth (Adapt-Exp).
277 **B.** Stringent response status according to growth condition in Newman carrying P_{oppB}-*lacZ* reporter
278 (blue, left panel) and P_{cshA}-*lacZ* (pink, right panel). β-gal activities of samples in SerFA (exponential
279 growth; Exp, A_{600} = ~1.5) and SerFA-Tric (Latency, A_{600} = ~0.3) are measured after 3 h growth. β-gal
280 activities were measured on 17 h samples in SerFA-Tric (exponential growth; Adapt-Exp, A_{600} = ~1.5).
281 Means of three independent cultures with standard errors (SE; not visible for BHI growth) are shown
282 for each experiment.

283

284

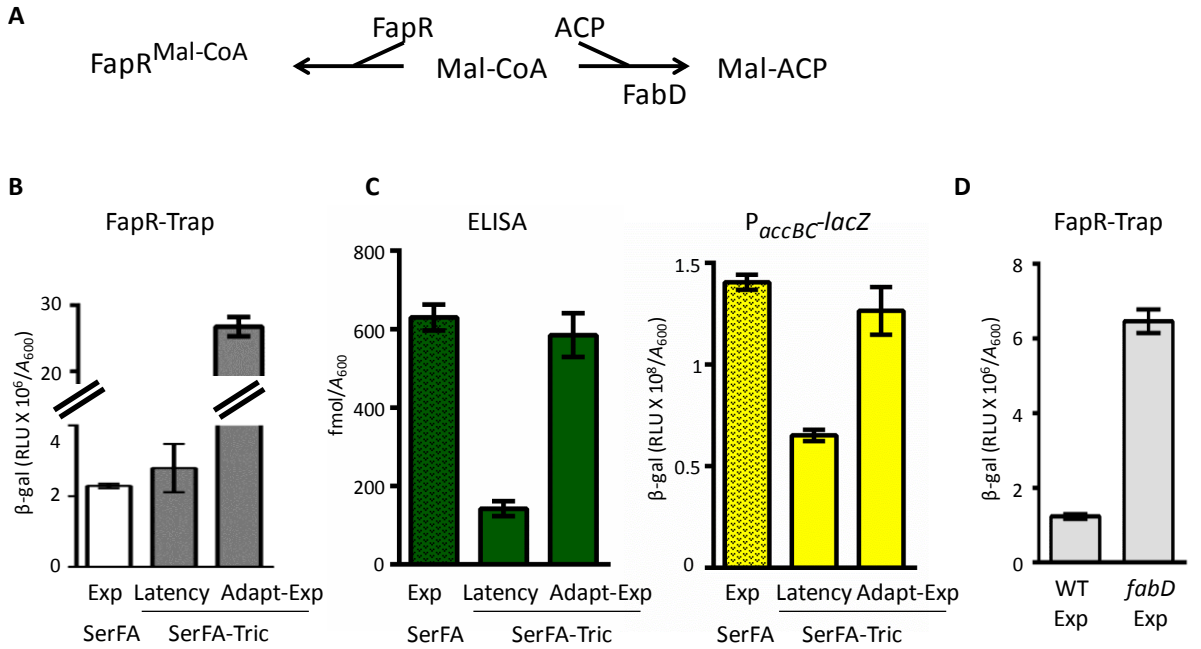

285

286

287 **Fig. 3. Shifts in malonyl-CoA distribution during anti-FASII adaptation. A.** The diagram illustrates the
288 two known malonyl-CoA interactants, FapR and FabD. Malonyl-CoA binds FapR (left), leading to FapR
289 derepression. Malonyl-CoA is also a FabD substrate (right). **B.** Assessment of FapR-bound malonyl-
290 CoA. FASII-antibiotic-adapted *S. aureus* display altered malonyl-CoA distribution. Newman expressing
291 FapR-Trap was grown in non-selective (SerFA) and anti-FASII (SerFA-Tric) media. β-gal activities were
292 measured in SerFA at A_{600} = ~2.0 (exponential growth: Exp, white), and in SerFA-Tric (dark grey)
293 during latency after 3 h growth A_{600} = ~0.3 (Latency) and upon adaptive exponential outgrowth at 17
294 h, A_{600} = ~2 (Adapt-Exp). **C.** Assessment of malonyl-CoA pools. *S. aureus* Newman cultures were
295 grown as in "**B**". Left panel: Sandwich ELISA assay (green) was used to measure total malonyl-CoA
296 (Materials and Methods). Right panel: P_{accBC}-*lacZ* reporter activity (yellow). **D.** Assessment of FapR-
297 bound malonyl-CoA in a *fabD* mutant using FapR-Trap. β-gal assays of Newman and *fabD* mutant
298 (CondT^R-17, a point mutant [4]) carrying FapR-Trap were performed in SerFA after 3 h growth with A_{600}
299 = ~1.0 (Exp; light grey). For each panel are shown the means and standard errors of three
300 independent experiments.

301

302

A

```
fabH fabF            -70 GAGTTTAAAAAGTAATCTATGATAAATTAATACCTGGTATTAAAAAATTTTATTAAGAAGGTGTTCAACT  -1
fapR plsX fabD fabG  -61 AAAGTGTTATGATATGTGAGGAATGTTTAAGACTAGGTACTAAAAAATGAGGGGTGAGACGTTGAAACTA  +9
fabI                -109 ATCAAACATTTATCGTTGTAATACGTTTAAATAACTTTATTAAAAAGTCATAATAGTGTTAAAATGTATT -39
plsC                 -42 AAATCTAGTTGTTATAAACAAATAAGTTAAGTAGGTGGCACAATGTATTCAGTGATTAGTAAGATTTTGA +28
Consensus                                            TTAANWCNNGGTAYTAA
```

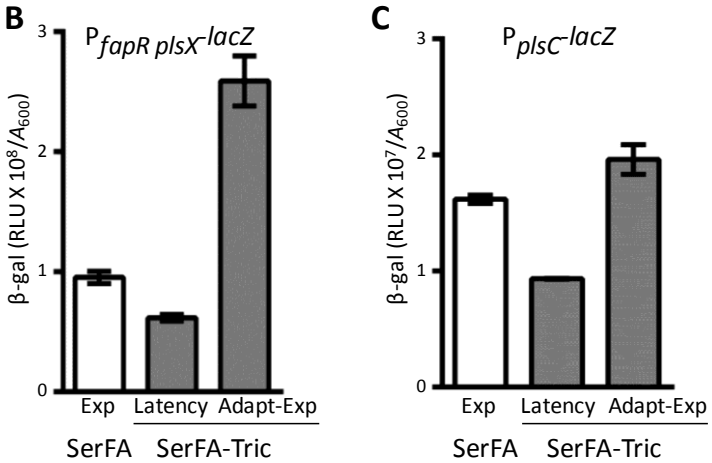

303

304

305 **Fig. 4. Expression of PlsX and PlsC in FASII-antibiotic-induced latency and adaptation. A.** Sequence
306 alignment of FapR binding sites in *S. aureus* N315 using the RegPrecise database [13,34]. Positions
307 correspond to the predicted start codon of the first Orf in each operon. Consensus nucleotides in the
308 17 bp FapR binding sequence are shaded. In the consensus sequence below the alignment: N, any
309 nucleotide; W, A or T; Y, T or C. Putative -10 RNA polymerase binding sites are underlined (from [13]).
310 The PlsC ATG and FapR TTG start sites are in italics. **B**, **C.** Shifts in *plsX* and *plsC* expression during
311 growth in non-selective (SerFA) and anti-FASII (SerFA-Tric) media. β-gal activities of *S. aureus*
312 Newman expressing $P_{fapR\ plsX}$-*lacZ* and P_{plsC}-*lacZ* are shown for samples processed in SerFA at OD_{600} =
313 ~2.0 (exponential phase, Exp), and in SerFA-Tric after 3h in latency (OD_{600} = ~0.3) and upon adaptive
314 exponential outgrowth at 17 h (OD_{600} = ~2.0; Adapt-Exp). Non-selective growth, white; selective
315 growth, dark grey. For each panel are shown the means and standard errors of three independent
316 experiments.

317

318

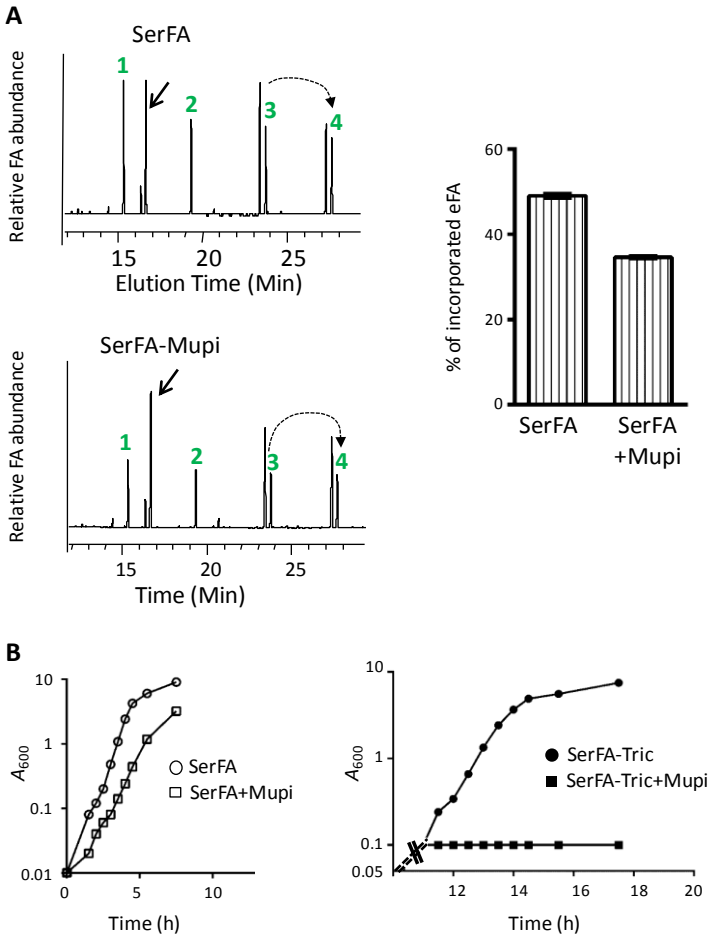

319

320

321 **Fig. 5. Subinhibitory mupirocin addition inhibits *S. aureus* eFA incorporation in membrane**
322 **phospholipids and synergizes with anti-FASII to inhibit adaptation. A,** Left, Fatty acid profiles of *S.*
323 *aureus* Newman grown in SerFA and SerFA+mupirocin (Mupi). Samples were processed after 3 h
324 growth. Black arrow, position of the main endogenous fatty acid *ai*15:0. eFA are; 1- C14:0; 2- C16:0;
325 3- C18:1; 4- C20:1 (elongation of C18:1). Dashed arrow, elongation of C18:1 (n+2). Right, percent eFA
326 of Newman grown in SerFA without and with Mupi, derived from integration of fatty acid profiles. **B.**
327 Left, *S. aureus* Newman cultures were grown in SerFA and SerFA+Mupi, or right, in SerFA-Tric and
328 SerFA-Tric+Mupi. Growth was monitored by A_{600}. Growth curves at right are shown starting at 10 h.
329 Mupi was used at 0.05 µg/ml. Results are representative of three independent experiments.

330

331

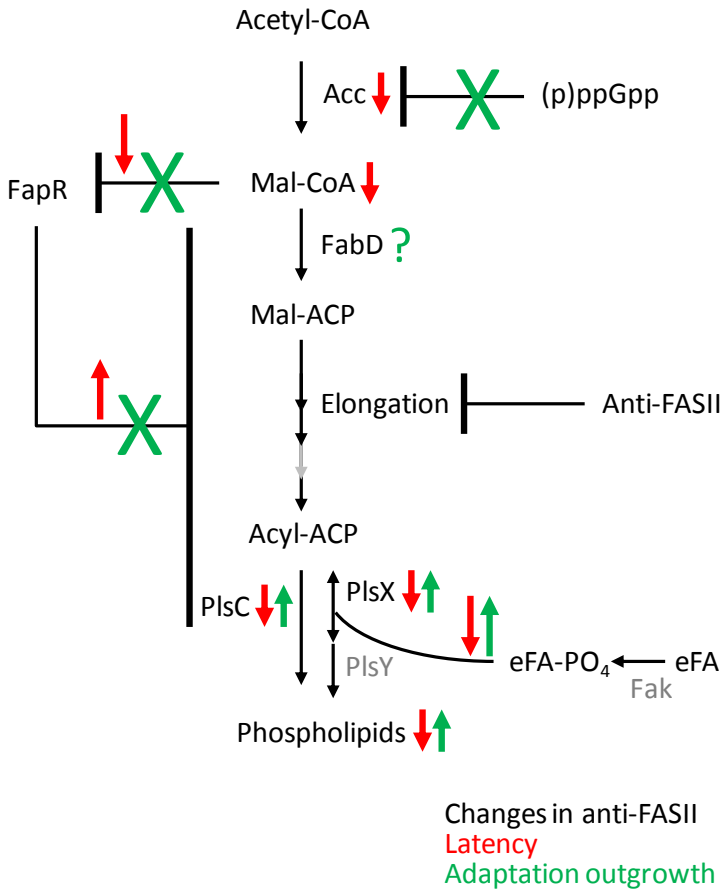

332

333

334 **Fig.6. Proposed contribution of (p)ppGpp in *S. aureus* adaptation to FASII antibiotics *via***
335 **intracellular malonyl-CoA (mal-CoA) pool distribution.** New findings of this study are in color: Red,
336 effects of anti-FASII-induced latency phase; green, effects during anti-FASII adaptation outgrowth.
337 Repression, lines with thick flat-end bar. FapR-mediated repression (flat-end thick line, Ч-shape)
338 covers functions indicated at right of the vertical thick flat-end bar. Note that mal-CoA binding to
339 FapR alleviates FapR repression [13]. "X", repression is alleviated. Up and down arrows, respectively
340 increased and decreased products in the color-coded condition. ACC, acetyl-CoA carboxylase; ACP,
341 acyl carrier protein. Fak, fatty acid kinase [35], grey, functions not measured. Only FASII enzymes
342 relevant to the model are indicated. "FabD ?", based on results, we propose that in adaptation
343 outgrowth, FabD cannot interact with mal-CoA. Anti-FASII induces (p)ppGpp, which leads to *acc*
344 repression. Less mal-CoA produced leaves FapR in repressor mode, down-regulating FASII and
345 phospholipid synthesis genes. During adaptation outgrowth, stringent response is reduced, and
346 increased mal-CoA alleviates FapR regulon repression, leading to incorporation of exogenous fatty
347 acids (eFA) in both membrane phospholipid positions [5].

348

349 **References:**

350

351 1 Uchil, R. R., Kohli, G. S., Katekhaye, V. M. & Swami, O. C. Strategies to combat antimicrobial
352 resistance. *J Clin Diagn Res* **8**, ME01-04, doi:10.7860/JCDR/2014/8925.4529 (2014).
353 2 Lu, H. & Tonge, P. J. Inhibitors of FabI, an enzyme drug target in the bacterial fatty acid
354 biosynthesis pathway. *Acc Chem Res* **41**, 11-20, doi:10.1021/ar700156e (2008).
355 3 Brinster, S. *et al.* Type II fatty acid synthesis is not a suitable antibiotic target for Gram-
356 positive pathogens. *Nature* **458**, 83-86, doi:10.1038/nature07772 (2009).
357 4 Morvan, C. *et al.* Environmental fatty acids enable emergence of infectious *Staphylococcus*
358 *aureus* resistant to FASII-targeted antimicrobials. *Nat Commun* **7**, 12944,
359 doi:10.1038/ncomms12944 (2016).
360 5 Kenanian, G. *et al.* Permissive Fatty Acid Incorporation Promotes Staphylococcal Adaptation
361 to FASII Antibiotics in Host Environments. *Cell Rep* **29**, 3974-3982 e3974,
362 doi:10.1016/j.celrep.2019.11.071 (2019).
363 6 Wang, J. *et al.* Platensimycin is a selective FabF inhibitor with potent antibiotic properties.
364 *Nature* **441**, 358-361, doi:10.1038/nature04784 (2006).
365 7 Banevicius, M. A., Kaplan, N., Hafkin, B. & Nicolau, D. P. Pharmacokinetics,
366 pharmacodynamics and efficacy of novel FabI inhibitor AFN-1252 against MSSA and MRSA in
367 the murine thigh infection model. *J Chemother* **25**, 26-31,
368 doi:10.1179/1973947812Y.0000000061 (2013).
369 8 Escaich, S. *et al.* The MUT056399 inhibitor of FabI is a new antistaphylococcal compound.
370 *Antimicrob Agents Chemother* **55**, 4692-4697, doi:10.1128/AAC.01248-10 (2011).
371 9 Feng, Z., Chakraborty, D., Dewell, S. B., Reddy, B. V. & Brady, S. F. Environmental DNA-
372 encoded antibiotics fasamycins A and B inhibit FabF in type II fatty acid biosynthesis. *J Am*
373 *Chem Soc* **134**, 2981-2987, doi:10.1021/ja207662w (2012).
374 10 Pishchany, G. *et al.* Amycomicin is a potent and specific antibiotic discovered with a targeted
375 interaction screen. *Proc Natl Acad Sci USA* **115**, 10124-10129, doi:10.1073/pnas.1807613115
376 (2018).
377 11 Parsons, J. B., Frank, M. W., Subramanian, C., Saenkham, P. & Rock, C. O. Metabolic basis for
378 the differential susceptibility of Gram-positive pathogens to fatty acid synthesis inhibitors.
379 *Proc Natl Acad Sci USA* **108**, 15378-15383, doi:10.1073/pnas.1109208108 (2011).
380 12 Gloux, K. *et al.* Clinical Relevance of Type II Fatty Acid Synthesis Bypass in *Staphylococcus*
381 *aureus*. *Antimicrob Agents Chemother* **61**, doi:10.1128/AAC.02515-16 (2017).
382 13 Albanesi, D. *et al.* Structural basis for feed-forward transcriptional regulation of membrane
383 lipid homeostasis in *Staphylococcus aureus*. *PLoS Pathog* **9**, e1003108,
384 doi:10.1371/journal.ppat.1003108 (2013).
385 14 Albanesi, D. & de Mendoza, D. FapR: From Control of Membrane Lipid Homeostasis to a
386 Biotechnological Tool. *Front Mol Biosci* **3**, 64, doi:10.3389/fmolb.2016.00064 (2016).
387 15 Ruch, F. E. & Vagelos, P. R. The isolation and general properties of *Escherichia coli* malonyl
388 coenzyme A-acyl carrier protein transacylase. *J Biol Chem* **248**, 8086-8094 (1973).
389 16 Nazir, A. & Harinarayanan, R. (p)ppGpp and the bacterial cell cycle. *J Biosci* **41**, 277-282
390 (2016).
391 17 Potrykus, K. & Cashel, M. (p)ppGpp: still magical? *Annu Rev Microbiol* **62**, 35-51,
392 doi:10.1146/annurev.micro.62.081307.162903 (2008).
393 18 My, L. *et al.* Transcription of the *Escherichia coli* fatty acid synthesis operon fabHDG is
394 directly activated by FadR and inhibited by ppGpp. *J Bacteriol* **195**, 3784-3795,
395 doi:10.1128/JB.00384-13 (2013).
396 19 Janssen, H. J. & Steinbuchel, A. Fatty acid synthesis in *Escherichia coli* and its applications
397 towards the production of fatty acid based biofuels. *Biotechnol Biofuels* **7**, 7,
398 doi:10.1186/1754-6834-7-7 (2014).

399 20 Pulschen, A. A. *et al.* The stringent response plays a key role in *Bacillus subtilis* survival of
400 fatty acid starvation. *Mol Microbiol* **103**, 698-712, doi:10.1111/mmi.13582 (2017).
401 21 Vadia, S. *et al.* Fatty Acid Availability Sets Cell Envelope Capacity and Dictates Microbial Cell
402 Size. *Curr Biol* **27**, 1757-1767 e1755, doi:10.1016/j.cub.2017.05.076 (2017).
403 22 Greenwood, R. C. & Gentry, D. R. The effect of antibiotic treatment on the intracellular
404 nucleotide pools of *Staphylococcus aureus*. *FEMS Microbiol Lett* **208**, 203-206,
405 doi:10.1111/j.1574-6968.2002.tb11082.x (2002).
406 23 Rhee, H. W. *et al.* Selective fluorescent chemosensor for the bacterial alarmone (p)ppGpp. *J*
407 *Am Chem Soc* **130**, 784-785, doi:10.1021/ja0759139 (2008).
408 24 Geiger, T. *et al.* The stringent response of *Staphylococcus aureus* and its impact on survival
409 after phagocytosis through the induction of intracellular PSMs expression. *PLoS Pathog* **8**,
410 e1003016, doi:10.1371/journal.ppat.1003016 (2012).
411 25 Polakis, S. E., Guchhait, R. B. & Lane, M. D. Stringent control of fatty acid synthesis in
412 *Escherichia coli*. Possible regulation of acetyl coenzyme A carboxylase by ppGpp. *J Biol Chem*
413 **248**, 7957-7966 (1973).
414 26 Reiss, S. *et al.* Global analysis of the *Staphylococcus aureus* response to mupirocin.
415 *Antimicrob Agents Chemother* **56**, 787-804, doi:10.1128/AAC.05363-11 (2012).
416 27 Schujman, G. E., Paoletti, L., Grossman, A. D. & de Mendoza, D. FapR, a bacterial
417 transcription factor involved in global regulation of membrane lipid biosynthesis. *Dev Cell* **4**,
418 663-672 (2003).
419 28 Feher, T., Libis, V., Carbonell, P. & Faulon, J. L. A Sense of Balance: Experimental Investigation
420 and Modeling of a Malonyl-CoA Sensor in *Escherichia coli*. *Front Bioeng Biotechnol* **3**, 46,
421 doi:10.3389/fbioe.2015.00046 (2015).
422 29 Ellis, J. M. & Wolfgang, M. J. A genetically encoded metabolite sensor for malonyl-CoA. *Chem*
423 *Biol* **19**, 1333-1339, doi:10.1016/j.chembiol.2012.08.018 (2012).
424 30 Johnson, A. O. *et al.* Design and application of genetically-encoded malonyl-CoA biosensors
425 for metabolic engineering of microbial cell factories. *Metab Eng* **44**, 253-264,
426 doi:10.1016/j.ymben.2017.10.011 (2017).
427 31 Rajamuthiah, R. *et al.* A Defensin from the Model Beetle Tribolium castaneum Acts
428 Synergistically with Telavancin and Daptomycin against Multidrug Resistant *Staphylococcus*
429 *aureus*. *PLoS One* **10**, e0128576, doi:10.1371/journal.pone.0128576 (2015).
430 32 Kizer, L., Pitera, D. J., Pfleger, B. F. & Keasling, J. D. Application of functional genomics to
431 pathway optimization for increased isoprenoid production. *Appl Environ Microbiol* **74**, 3229-
432 3241, doi:10.1128/AEM.02750-07 (2008).
433 33 Kumari, R., Saxena, R., Tiwari, S., Tripathi, D. K. & Srivastava, K. K. Rv3080c regulates the rate
434 of inhibition of mycobacteria by isoniazid through FabD. *Mol Cell Biochem* **374**, 149-155,
435 doi:10.1007/s11010-012-1514-5 (2013).
436 34 Novichkov, P. S. *et al.* RegPrecise 3.0--a resource for genome-scale exploration of
437 transcriptional regulation in bacteria. *BMC Genomics* **14**, 745, doi:10.1186/1471-2164-14-745
438 (2013).
439 35 Parsons, J. B. *et al.* Identification of a two-component fatty acid kinase responsible for host
440 fatty acid incorporation by *Staphylococcus aureus*. *Proc Natl Acad Sci USA* **111**, 10532-10537,
441 doi:10.1073/pnas.1408797111 (2014).

442

Supplementary information

(p)ppGpp and malonyl-CoA set the pace for *Staphylococcus aureus* adaptation to FASII antibiotics and provide a basis for bi-therapy inhibition

Amit Pathania[1*], Jamila Anba-Mondoloni[1], David Halpern[1], Laëtitia Dupont[1], Gilles Lamberet[1], Patrick Trieu-Cuot [2], Karine Gloux[1] and Alexandra Gruss[1*]

[1]Micalis Institute, INRAE, AgroParisTech, Université Paris-Saclay, Jouy en Josas, France, [2] Unité de Biologie des Pathogènes à Gram-positif, CNRS UMR 2001, Institut Pasteur, Paris, France

13 **Materials and Methods**

14

15 **Strains and media.**

16 Newman [1], RN4220 [2] and USA300 [3] strains of *S. aureus* were used in this study. *E. coli* strains DH5α [4]
17 and IM08B [5] were used for cloning. BHI (Brain Heart Infusion) and LB (Luria-Bertani) media were used
18 respectively for *S. aureus* and *E. coli* growth. *S. aureus* precultures were routinely prepared in BHI
19 medium. Three fatty acids (C14:0; myristic acid, C16:0; palmitic acid and C18:1; oleic acid;, Larodan
20 Fine Chemicals, Sweden) were prepared as 100 mM stocks in DMSO and used at final equimolar
21 concentrations of 0.17 mM each in experiments (referred as eFA). Ser-FA (BHI containing eFA+10%
22 newborn calf serum; Sigma) and SerFA-Tric (SerFA+Triclosan 0.5 µg/ml) were the modified media
23 used as indicated. Antibiotics kanamycin (50 µg/ml) and erythromycin (5 µg/ml) were used in *E. coli*
24 and *S. aureus* respectively to select pTCV-*lac*-based reporter fusion plasmids [6]. Antibiotic adaptation
25 experiments with plasmid-carrying strains were done in SerFA-Tric containing 2 µg/ml erythromycin;
26 note that the latency period was extended by about 4-6 h in this condition. Mupirocin (Sigma), a
27 functional analogue of isoleucyl-AMP and a stringent response inducer of (p)ppGpp [7] was prepared in
28 DMSO and used at 0.1 µg/ml [8,9] to validate (p)ppGpp sensors, or at 0.05 µg/ml when used in
29 combination with anti-FASII. Equal volumes of DMSO were added to control samples when mupirocin
30 was used.

31 **Construction of reporter fusions.**

32 Promoter regions of *oppB*, *ilvD*, *cshA*, as well as *fapR*, *plsC* and *accBC*, were cloned in pTCV-*lac*
33 plasmid (Table S1) using the appropriate primers (Table S6). PCR-amplified DNA fragments and
34 plasmid were treated with restriction enzymes EcoRI and BamH1 and ligated products were
35 transformed into DH5α or IM08B. The obtained constructs were confirmed by DNA sequencing.
36 Plasmids obtained from IM08B were used directly to transform the *S. aureus* Newman strain; clones
37 obtained in DH5α were first passaged through RN4220. A standard electroporation protocol was
38 used to transform DNA in *S. aureus* [10].

39 **(p)ppGpp sensors.**

40 *oppB* (NWMN_0856) and ilvD (NWMN_1960) are up-regulated, and *cshA* (NWMN_1985) genes is
41 down- regulated upon stringent response induction [7,11,12]. The corresponding stringent response
42 sensors P_{oppB}-*lacZ*, P_{ilvD}-lacZ and P_{cshA}-*lacZ* (Table S1) were tested in medium containing 0.1 µg/ml
43 mupirocin [7], and validated as *bone fide* (p)ppGpp sensors (Fig. 1A, Table S4).

44

45 **FapR activity sensor.**

46 To estimate malonyl-CoA pools bound to FapR, we designed a transcriptional fusion with promoter
47 and operator sequences containing a consensus FapR binding site; FapR-Trap (Fig. S2, Table S1). The
48 construction was based on similar studies done previously to estimate malonyl-CoA pools [13,14].

49 **β-galactosidase (β-gal) assay.**

50 Fresh cultures were prepared at A_{600} = 0.1 from overnight BHI cultures and β-gal activities were
51 measured at the indicated A_{600} times. When mupirocin was used, cultures were treated or not at A_{600}
52 = 0.1 and processed 1 h later. All samples of a set were stored at -20°C prior to measurements, which
53 were performed for all samples of a same set. β-gal activities were measured as described [15], except
54 that samples derived from SerFA-containing medium were incubated with lysostaphin (0.1 mg/ml)
55 for 30 min at room temperature prior to processing with β-Glo™ reagents (Promega). β-gal values
56 (mean ± standard error) were determined from three independently performed experiments.

57 **Malonyl-CoA measurement by ELISA assay.**

58 Bacterial cultures were prepared as above, and samples were processed at the indicated A_{600}/time
59 interval according to our test conditions. For each sample, the equivalent of A_{600} = 30 was centrifuged
60 at 8,000 rpm at room temperature for 5 min. Pelleted cells were immediately frozen in liquid
61 nitrogen and transferred to -80°C overnight. Ice cold PBS (Phosphate Buffer Saline) was used to
62 resuspend cells at 4°C, which were then sonicated in FastPrep (MP Biomedicals). Supernatants were
63 collected by centrifuging the cell slurry at 13,000 rpm at 4°C for 5 min, and stored at -80°C until use.
64 ELISA tests for total malonyl-CoA measurements were performed as per manufacturer's instructions
65 (CUSABIO). Malonyl-CoA standards were run along with test samples. Each experiment was
66 performed on three independent cultures. Mean values ± standard errors are presented.

67 For malonyl-CoA measurements under stringent response conditions (Fig. 1C, left panel),
68 Newman was first grown in BHI to A_{600} of 0.5 from an initial inoculum of 0.01. Cultures were treated
69 or not with 0.1 µg/ml mupirocin for 30 minutes (A_{600} = ~1 for both samples). ELISA assays were
70 performed as above.

71 **Determination of *S. aureus* fatty acid profiles**.

72 Fatty acid profiles were done as described [16]. Newman pre-cultures prepared from two independent
73 colonies were diluted to A_{600} = 0.1 in SerFA and grown 3 h with and without mupirocin (0.05 µg/ml).
74 A_{600} of SerFA samples were ~2.5 and treated samples ~1.0**.** Percentage of eFA are shown (mean ±
75 standard errors).

76

77 **Supplementary Figures and Tables**

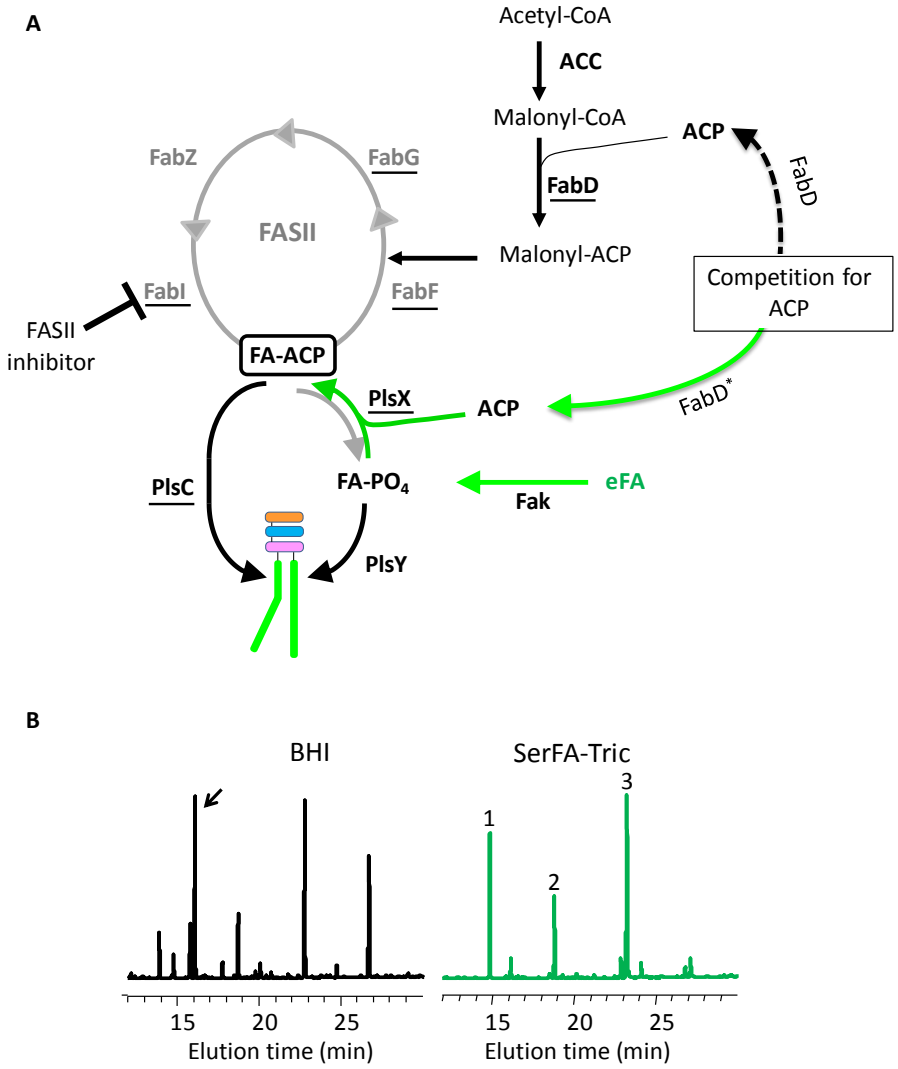

78

79

80 **Fig. S1. *S. aureus* bypasses FASII inhibition by exogenous fatty acid (eFA) incorporation in**
81 **membrane phospholipids. A.** Model for anti-FASII adaptation. FASII and FASII bypass are
82 schematized as characterized; functions whose expression is controlled by FapR repressor are
83 underlined [16-19]. eFA phosphorylation by Fak (fatty acid kinase) [20] provides an intermediate that may
84 either be incorporated in position 1 of the glycerol-3-phosphate backbone *via* PlsY, or act as a
85 substrate for PlsX to then be incorporated in position 2 via PlsC. In the absence of serum, FabD
86 (malonyl-CoA:ACP transacylase) mutations promote anti-FASII adaptation [16]. In contrast, serum
87 favors FASII antibiotic adaptation without FASII mutations [21]. **B.** Fatty acid profiles of *S. aureus*
88 Newman. Left, BHI grown cells; right, cells grown overnight in SerFA-Tric. Cultures started at A_{600} =
89 0.01 were harvested at A_{600} = 1. Arrow indicates *anteiso* 15 (*ai*15), the major fatty acid synthesized by
90 *S. aureus*. eFA: 1, C14:0; 2, C16:0; 3, C18:1. Profiles are representative of three independent
91 experiments. FA, fatty acids; FA-ACP, fatty acyl-ACP; FA-PO_4, acyl-phosphate; grey, inhibited pathway.
92 FabD*, mutated or inhibited enzymes.

93

94

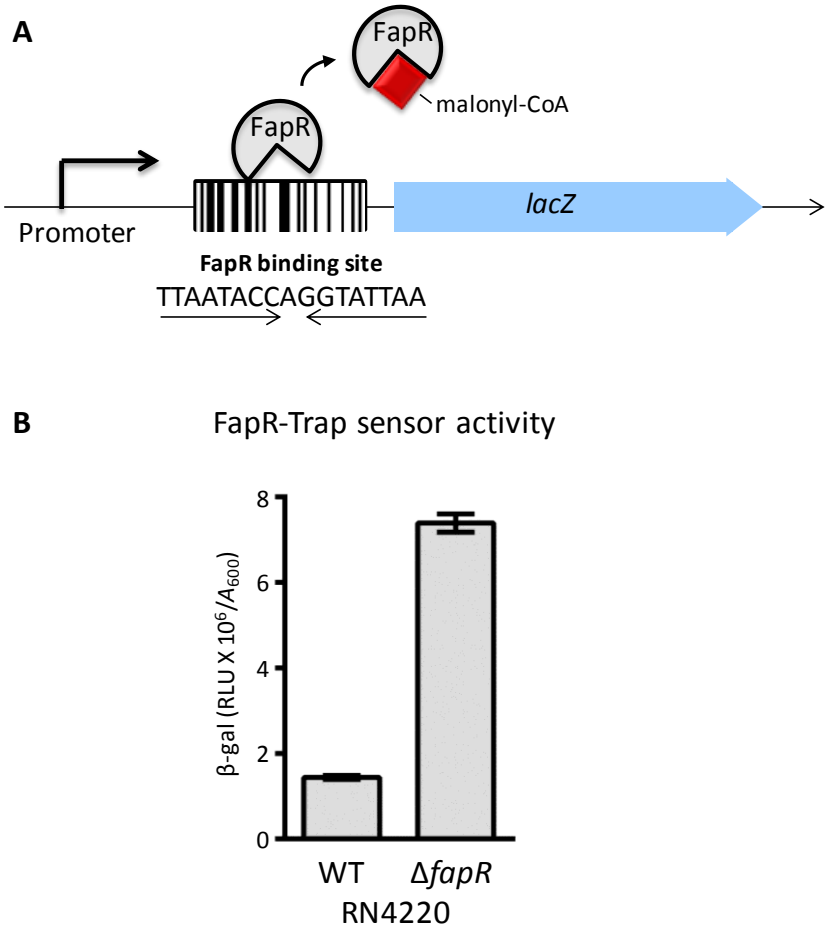

95

96

97 **Fig. S2. FapR-Trap, a malonyl-CoA sensor based on FapR operon *lacZ* fusion. A.** Schematic design of
98 FapR-Trap (pJJ004, Table S1). Malonyl-CoA (red diamond) binds FapR (pacman) leading to its release
99 from the FapR binding site (bar code) and expression of *lacZ* (blue) to produce β-galactosidase. The
100 17 bp FapR consensus binding site used in the construction is shown (based on [17]); converging arrows
101 indicate the 8 bp inverted repeat. **B.** Validation of the FapR-Trap as sensor. β-gal assays were
102 performed with RN4220 and its Δ*fapR* derivative $RN4220_{\Delta fapR}$ [17] carrying FapR-Trap after 3 h growth
103 in SerFA.

104

105 **Table S1. Plasmid constructions** [a]

106

Plasmid	Description
pTCV-*lac*	Promoter expression vector comprising pACYC184 and pAMβ1 as replication origins functional in respectively Gram- negative and positive bacterial hosts [6].
pJJ004 **(FapR-Trap)**	pTCV-*lac* derivative in which *lacZ* transcription is driven by a synthetic promoter designed from the *fabH fabF* (NWMN_0853 and NWMN_0854) operon. An 81 bp hybrid primer-pair (FapRtrapfd and FapRtraprp) was cloned into pTCV-*lac* into EcoRI and BamHI sites. A consensus FapR binding site is present in the promoter (Fig. S2).
pJJ005 **(P_{ilvD}-*lacZ*)**	pTCV-*lac* derivative carrying *lacZ* fused to the promoter region of *ilvD-ilvB* (NWMN_1960 to NWMN_1961). A 515 bp fragment from -500 to +15 with respect to the *ilvD* start codon (genome positions 2168952-2169466) is cloned into pTCV-*lac* EcoRI-BamHI sites. The clone carries an A to G substitution at position-277. This nucleotide change is expected not to alter (p)ppGpp regulation.
pJJ006 **(P_{oppB}-*lacZ*)**	pTCV-*lac* derivative carrying *lacZ* fused to the promoter region of the *oppB oppC oppD oppF oppA* (NWMN_0856 to NWMN_0860) operon. A 514 bp fragment from -499 to +15 with respect to the *oppB* start codon (genome positions 950296-950809) is cloned into pTCV-*lac* EcoRI-BamHI sites.
pJJ008 **(P_{cshA}-*lacZ*)**	pTCV-*lac* derivative carrying *lacZ* fused to the *cshA* (NWMN_1985) promoter region. A 515 bp fragment from -500 to +15 with respect to the *cshA* start codon (genome positions 2207332-2207846) is cloned into pTCV-*lac* EcoRI-BamHI sites.
pJJ013 **($P_{fapR\ plsX}$-*lacZ*)**	pTCV-*lac* derivative carrying *lacZ* fused to the promoter region of the *fapR plsX fabD fabG* (NWMN_1138 to NWMN_1141) operon. A 315 bp fragment from -300 to +15 with respect to the start codon (genome positions 1247750-1248064) of the operon is cloned into pTCV-*lac* EcoRI-BamHI sites.
pJJ019 **(P_{plsC}-*lacZ*)**	pTCV-*lac* derivative carrying *lacZ* fused to the *plsC* (NWMN_1620) promoter region. A 315 bp fragment from -300 to +15 with respect to the *plsC* start codon (genome positions 1799913-1800227) is cloned into pTCV-*lac* EcoRI-BamHI sites.
pJJ027 **(P_{accBC}-*lacZ*)**	pTCV-*lac* derivative carrying *lacZ* fused to the promoter region of the *accB accC* (NWMN_1432, NWMN_1431) operon. Hybrid primer-pair of 103 bp (accBCfp and accBCrp), corresponding to genome positions 1604036-1603934**,** was used to clone the promoter region upstream of *accB* into pTCV-*lac* into EcoRI and BamHI sites.

107

108 [a] Designations of promoter fusions are in bold (in parentheses). See Table S6 for primer pairs used for
109 clonings.

110

111 **Table S2. Stringent response signature in proteome of USA300 strain during FASII-antibiotic-**
112 **induced latency.**

113

Protein	Accession Number	Mupirocin transcriptome [a]	Proteome Ratio SerFA-Tric /SerFA [b]	Proteome p values [c]
30S Ribosomal				
S6 rpsF	WP_001261460.1	3-5	1.59	<0.05
S7 rpsG	WP_078055728.1	3-5	1.37	<0.05
S8 rpsH	WP_000178881.1	3-5	1.39	<0.05
S12 rpsL	WP_001142337.1	3-5	1.45	<0.05
S13 rpsM	WP_000090796.1	3-5	1.45	<0.05
S15 rpsO	WP_001018328.1	3-5	1.79	<0.05
S18 rpsR	WP_000897044.1	2-3	1.64	<0.05
S19 rpsS	WP_000124353.1	2-3	2	<0.05
50S Ribosomal				
L5 rplE	WP_001080824.1	3-5	1.6	<0.05
L6 rplF	WP_000091975.1	3-5	1.3	<0.05
L10 rplJ	WP_001273085.1	5-10	1.4	<0.05
L11 rplK	WP_001085792.1	3-5	1.75	<0.05
L13 rplM	WP_001250038.1	5-10	1.67	<0.05
L15 rplO	WP_000766074.1	5-10	1.5	<0.05
L16 rplP	WP_000926310.1	5-10	1.5	<0.05
L18 rplR	WP_000623881.1	3-5	1.37	<0.05
Amino acid synthesis				
ThrC	WP_001255460.1	5-10	2.2	<0.1 [d]
Stress response				
UspA	WP_000634175.1	2-3	2.2	<0.1 [d]
Other				
CshA	WP_001178942.1	5-10	1.42	<0.05
GuaC	WP_000688126.1	10-20	2.6	<0.05
RuvA	WP_000271547.1	3-5	2.3	<0.05

114

115 [a] Transcriptional responses to subinhibitory mupirocin (0.03 µg/ml) are as reported [11], and presented
116 here as ratios of mupirocin- treated/non-treated samples. [b] Proteomic responses to triclosan during
117 the anti-FASII-induced latency phase as reported for USA300 *spa::Tn* (JE2) [3,21]. [c] Median values of
118 corresponding peptide reads done in quadruplicate are used to calculate the proteome ratio. p
119 values are calculated by Mann-Whitney method for one-tailed assay by GraphPad Prism. [d] p values
120 not statistically significant but trend with expression pattern. Proteomics data of responses to
121 SerFA-Tric is stored in the Mendeley database (doi:10.17632/9292c75797.2). Red, fold-negative
122 values; green,fold-positive values.

123

124 **Table S3. Total and proportion of FapR-bound malonyl-CoA depends on growth condition.**

125

	Relative proportions [a]		% Malonyl-CoA bound to FapR
	Total Malonyl-CoA pools	FapR-Trap	
Non- selective [b]	100	8	8%
Anti-FASII [c] Latency	23	10	43 %
Anti-FASII [c] Adapted- Exponential	93	100	108 %

126

127 [a] Relative proportions of total and FapR-bound malonyl-CoA from Fig. 3B and 3C are determined
128 based on the highest obtained value for respective measurements (indicated as 100 %). [b] Medium
129 was SerFA. [c] FASII inhibitor triclosan is added to SerFA (SerFA-Tric).

130

131 **Table S4. Responses of FapR regulon genes and known stringent response induced genes to**
132 **mupirocin.**

133

	Promoter fusion	Mupirocin/ No addition [a]	Effect
Control	Pctl [b]	1.1 ± 0.03	None
Stringent response	P_{ilvD}-*lacZ*	2.1 ± 0.42	Stimulation
	P_{oppB}-*lacZ*	1.87 ± 0.69	Stimulation
	P_{cshA}-*lacZ*	0.33 ± 0.06	Repression
FapR regulon	P_{accBC}-*lacZ*	0.25 ± 0.04	Repression
	$P_{fapR\ plsX}$-*lacZ*	0.25 ± 0.03	Repression
	P_{plsC}-*lacZ*	0.34 ± 0.06	Repression

134

135 [a] Measurements (standard deviation) were determined on three independent samples in BHI
136 medium containing or not mupirocin 0.1 µg/ml (described in Materials and Methods). Experiments
137 were performed independently from those presented in Fig. 1. [b] Pctl corresponds to the plasmid
138 vector pTCVlac [6], lacking a *lacZ* promoter.

139

140 **Table. S5.** Subinhibitory mupirocin treatment synergizes with AFN-1252 to inhibits MRSA USA300
141 growth [a].

142

Media	A_{600} at 16 h
SerFA	11.4 ±0.3
SerFA+AFN-1252 [b]	11.1 ±0.7
SerFA + Mupirocin	6.3 ±1.7
SerFA-AFN-1252+Mupirocin	0.2 ±0.06

143

144 [a] Mupirocin was used at 0.06 µg/ml, AFN-1252 at 0.5 µg/ml. The USA300_FRPR3757 strain is MRSA
145 (methicillin resistant *S. aureus*). It was precultured in SerFA medium, and diluted 1:100 in SerFA
146 containing or not mupirocin and AFN-1252. A_{600} optical densities were determined after 16 h aerobic
147 growth at 37°C. Results shown are the average (range) of 2 independent experiments. [b] AFN-1252 is
148 a pipeline antibiotic that, like triclosan, targets FabI [22].

149

150 **Table S6.** Primers

151

Primer ID	Sequence of Primer (5'to 3')[a]
FapRtrapfd	AATTCTCCTACGACAATATCCT**TTGCAT**TTAAAGTATCTAAAATC**TATGAT**AAA***TTAATACCTGGTATTA A***AAATATTTATTAGAAG *pJJ004 (FapR-Trap)*
FapRtraprp	GATCCTTCTAATAAATATTT***TTAATACCAGGTATTAA***TTT**ATCATA**GATTTTAGATACTTTAA**ATGCAA**A GGATATTGTCGTAGGAG *pJJ004 (FapR-Trap)*
ilvDfp	TTGCCGGAATTCCCTATATTATGCTTTTCATTCA *pJJ005 (P_{ilvD}-lacZ)*
ilvDrp	CTAGCGGGATCCTTACATGTCGCTTCGCATAGT *pJJ005 (P_{ilvD}-lacZ)*
OppBfp	TTGCCGGAATTCTTGAAAAATGGATCATCAGA *pJJ006 (P_{oppB}-lacZ)*
OppBrp	CAAGCGGGATCCTTAAATATATTTCCCCATCTAA *pJJ006(P_{oppB}-lacZ)*
CshAfp	TTGCCGGAATTCCTTTTACTTATAAAAATGATTTG *pJJ008 (P_{cshA}-lacZ)*
CshArp	CAAGCGGGATCCTTATTTAAAATTTTGCAAAATAATTC *pJJ008 (P_{cshA}-lacZ)*
FapRfp	TTGCCGGAATTCCAGCTGAACTTATTCAATCTGG *pJJ013 ($P_{fapR\ plsX}$-lacZ)*
FapRrp	CAAGCGGGATCCTTACGTCTCACCCCTCATTTTTTAGT *pJJ013 ($P_{fapR\ plsX}$-lacZ)*
PlsCfp	TTGCCCGAATTCAAGTGCACCAATAATTCCAGCA *pJJ019 (P_{plsC}-lacZ)*
PlsCrp	CAAGCGGGATCCTTAAATCACTGAATACATTGTGCCACC *pJJ019 (P_{plsC}-lacZ)*
AccBCfp	AATTCGTCGCCAGCAATATGAACATGC**TTGAAT**TGAAGAGTTGTCTCAAG**TAAAAT**AGACGGGTAGAT GAAAACAAACTGAAGGAGTCAGTAATAATGAACTTTAAAG *pJJ027 (P_{accBC}-lacZ)*
AccBCrp	GATCCTTTAAAGTTCATTATTACTGACTCCTTCAGTTTGTTTTCATCTACCCGTCT**ATTTTA**CTTGAGACA ACTCTTCA**ATTCAA**GCATGTTCATATTGCTGGCGACG *pJJ027 (P_{accBC}-lacZ)*

152

153 [a] Restriction sites are underlined; putative -10 and -35 motifs are in bold; FapR consensus binding site
154 is in italics.

155

156 **References:**

157 1 Herbert, S. *et al.* Repair of global regulators in *Staphylococcus aureus* 8325 and comparative
158 analysis with other clinical isolates. *Infect Immun* **78**, 2877-2889, doi:10.1128/IAI.00088-10
159 (2010).
160 2 Kreiswirth, B. N. *et al.* The toxic shock syndrome exotoxin structural gene is not detectably
161 transmitted by a prophage. *Nature* **305**, 709-712 (1983).
162 3 Fey, P. D. *et al.* A genetic resource for rapid and comprehensive phenotype screening of
163 nonessential *Staphylococcus aureus* genes. *MBio* **4**, e00537-00512, doi:10.1128/mBio.00537-
164 12 (2013).
165 4 Sambrook, J. R. D. W. Molecular cloning: a laboratory manual. *3rd ed, Cold Spring Harbor*
166 *Laboratory, Cold Spring Harbor, NY.* (2001).
167 5 Monk, I. R., Tree, J. J., Howden, B. P., Stinear, T. P. & Foster, T. J. Complete Bypass of
168 Restriction Systems for Major *Staphylococcus aureus* Lineages. *MBio* **6**, e00308-00315,
169 doi:10.1128/mBio.00308-15 (2015).
170 6 Poyart, C. & Trieu-Cuot, P. A broad-host-range mobilizable shuttle vector for the construction
171 of transcriptional fusions to beta-galactosidase in gram-positive bacteria. *FEMS Microbiol Lett*
172 **156**, 193-198 (1997).
173 7 Reiss, S. *et al.* Global analysis of the *Staphylococcus aureus* response to mupirocin.
174 *Antimicrob Agents Chemother* **56**, 787-804, doi:10.1128/AAC.05363-11 (2012).
175 8 Rajamuthiah, R. *et al.* A Defensin from the Model Beetle Tribolium castaneum Acts
176 Synergistically with Telavancin and Daptomycin against Multidrug Resistant *Staphylococcus*
177 *aureus*. *PLoS One* **10**, e0128576, doi:10.1371/journal.pone.0128576 (2015).
178 9 Fernandez, C. *et al.* A double-blind, randomized, placebo-controlled clinical trial to evaluate
179 the safety and efficacy of mupirocin calcium ointment for eliminating nasal carriage of
180 *Staphylococcus aureus* among hospital personnel. *J Antimicrob Chemother* **35**, 399-408
181 (1995).
182 10 Kraemer, G. R. K. & Iandolo, J. J. High-frequency transformation of *Staphylococcus aureus* by
183 electroporation. *Current Microbiology* **21**, 373, doi:10.1007/BF02199440 (1990).
184 11 Geiger, T. *et al.* The stringent response of *Staphylococcus aureus* and its impact on survival
185 after phagocytosis through the induction of intracellular PSMs expression. *PLoS Pathog* **8**,
186 e1003016, doi:10.1371/journal.ppat.1003016 (2012).
187 12 Anderson, K. L. *et al.* Characterization of the *Staphylococcus aureus* heat shock, cold shock,
188 stringent, and SOS responses and their effects on log-phase mRNA turnover. *J Bacteriol* **188**,
189 6739-6756, doi:10.1128/JB.00609-06 (2006).
190 13 Ellis, J. M. & Wolfgang, M. J. A genetically encoded metabolite sensor for malonyl-CoA. *Chem*
191 *Biol* **19**, 1333-1339, doi:10.1016/j.chembiol.2012.08.018 (2012).
192 14 Johnson, A. O. *et al.* Design and application of genetically-encoded malonyl-CoA biosensors
193 for metabolic engineering of microbial cell factories. *Metab Eng* **44**, 253-264,
194 doi:10.1016/j.ymben.2017.10.011 (2017).
195 15 Lechardeur, D. *et al.* Discovery of intracellular heme-binding protein HrtR, which controls
196 heme efflux by the conserved HrtB-HrtA transporter in Lactococcus lactis. *J Biol Chem* **287**,
197 4752-4758, doi:10.1074/jbc.M111.297531 (2012).
198 16 Morvan, C. *et al.* Environmental fatty acids enable emergence of infectious *Staphylococcus*
199 *aureus* resistant to FASII-targeted antimicrobials. *Nat Commun* **7**, 12944,
200 doi:10.1038/ncomms12944 (2016).
201 17 Albanesi, D. *et al.* Structural basis for feed-forward transcriptional regulation of membrane
202 lipid homeostasis in *Staphylococcus aureus*. *PLoS Pathog* **9**, e1003108,
203 doi:10.1371/journal.ppat.1003108 (2013).
204 18 Zhang, Y. M. & Rock, C. O. Membrane lipid homeostasis in bacteria. *Nat Rev Microbiol* **6**, 222-
205 233, doi:10.1038/nrmicro1839 (2008).

19 Fujita, Y., Matsuoka, H. & Hirooka, K. Regulation of fatty acid metabolism in bacteria. *Mol Microbiol* **66**, 829-839, doi:10.1111/j.1365-2958.2007.05947.x (2007).

20 Parsons, J. B. *et al.* Identification of a two-component fatty acid kinase responsible for host fatty acid incorporation by *Staphylococcus aureus*. *Proc Natl Acad Sci U S A* **111**, 10532-10537, doi:10.1073/pnas.1408797111 (2014).

21 Kenanian, G. *et al.* Permissive Fatty Acid Incorporation Promotes Staphylococcal Adaptation to FASII Antibiotics in Host Environments. *Cell Rep* **29**, 3974-3982 e3974, doi:10.1016/j.celrep.2019.11.071 (2019).

22 Banevicius, M. A., Kaplan, N., Hafkin, B. & Nicolau, D. P. Pharmacokinetics, pharmacodynamics and efficacy of novel FabI inhibitor AFN-1252 against MSSA and MRSA in the murine thigh infection model. *J Chemother* **25**, 26-31, doi:10.1179/1973947812Y.0000000061 (2013).